Basic Numerical Simulation of Large-Scale Plume Activity Due to the Circum-Pacific Lithosphere Subduction and Implications for the Elementary Process Associated with the Static-Layered Terrestrial Mantle

By Takao EGUCHI, Mizuho ISHIDA, Kiyoshi MATSUBARA,
Takumi MURAKOSHI and Yasuyuki IWASE

Reprinted from the Memoirs of the National Defense Academy
Vol.57, No.1

September 2017

YOKOSUKA, JAPAN

Memoirs
of the National Defense Academy,
Japan, Vol. 57, No. 1,
(2017), pp. 1-10

<paper>

Basic Numerical Simulation of Large-Scale Plume Activity Due to the Circum-Pacific Lithosphere Subduction and Implications for the Elementary Process Associated with the Static-Layered Terrestrial Mantle

(Dedicated to Professor Kikuro TOMINE)

By Takao EGUCHI* Mizuho ISHIDA** Kiyoshi MATSUBARA***
Takumi MURAKOSHI **** and Yasuyuki IWASE ****

(Received: April 14, 2017; Accepted for publication: June 9, 2017)

Abstract.

To unveil the global dynamics of long-term lithosphere subduction along the circum-Pacific Ocean and relationship with large-scale mantle plume activity, we conducted 3-D spherical numerical simulations using a newly developed program. This program is based on the finite difference method with the Boussinesq (incompressible) approximation and temperature-dependent viscosity. To obtain a higher precision time integral, we adopted the Newton method. In addition, the preconditioned 'Bi-CGSTAB' (Bi-Conjugate Gradient Stabilized) method was incorporated to solve the Jacobian matrix of five finite difference equations for the velocity vector, pressure, and temperature. The preconditions used were matrix-matrix multiplication and incomplete LU factorization. We subsequently modeled circum-Pacific lithosphere subduction using the initial condition of a cool ring, at the base of the upper mantle along the equatorial great circle, imposed on the horizontally uniform temperature field with thermal boundary layers. The results indicated major upwellings at latitudes ± 30~40° as a response function. Secondary rising systems at both polar regions were clear. Our result numerically manifests part of the Green function-like elementary processes of large-scale passive flows within the static layered terrestrial mantle.

Keywords: Mantle Flow, Circum-Pacific Subduction Zone, Numerical Simulation

1. Introduction

To clarify the basic and fundamental nature of 3-D mantle convection dynamics, including unsteady or intermittent large-scale plume activity, we must conduct numerical simulations with various initial and boundary conditions, as well as constraints for rheology parameters, such as viscosity and temperature.

The main objective of this study is to characterize the response function of the simply shaped instantaneous anomaly incorporated in the earth's mantle.

However, we cannot analytically elucidate the response function due to the complexity of nonlinear equations for 3-D spherical convection. Runcorn[1], according to an analysis[2] of the critical Rayleigh number for discrete uniform-sized convection cells within 3-D various thickness fluid layers, demonstrated the basic pattern of mantle convection cells in the earth with a growing core. Runcorn[1], for example, suggests that in the case of a 3×10^3 km thick mantle, four uniform-sized convection cells along the cross section of each hemisphere is the most likely pattern, indicating that the diameter of the cell is $\sim 5 \times 10^3$ km. Runcorn[1], however, did not include calculation cases of point or great-circle sources with

* Professor; Department of Earth and Ocean Sciences, National Defense Academy
** Fellow at the National Research Institute for Earth Science and Disaster Prevention (NIED), 3-1, Ten-nodai, Tsukuba, Ibaraki 305-0006, JAPAN
*** AdvanceSoft Corporation, 4-3, Kandasurugadai, Chiyoda-ku, Tokyo 101-0062, JAPAN
**** Research Associate; Department of Earth and Ocean Sciences, National Defense Academy

anomalously low temperatures inserted within the horizontally uniformly layered thermal field.

The study of Runcorn[1] as well as of Chandrasekhar[2] should be re-evaluated with 3-D numerical calculations using recently advanced simulation technology. For example, using their code for 3-D spherical shell convection with the temperature dependent viscosity, Ratcliff et al. [3] numerically demonstrated the steady-state character of tetrahedral and cubic flow systems. We hypothesize that parameters for 3-D initial conditions assigned by Ratcliff et al.[3] for modeling the flow patterns can strongly constrain other flow patterns. In contrast, a set of initial conditions incorporated in this study is rather under-controlled compared to those in Ratcliff et al. [3]. More explicitly, for simple simulation studies as this one, the configuration of initial calculation parameters[3] appear over-controlled. Our goal is to reveal components of basic and fundamental behavior associated with the dynamic response of 3-D non-linear mantle flow systems.

On the current terrestrial earth surface, we can recognize the scattered locations of ascending mantle plumes, i.e., 'hotspots.' In addition, both the major zones of oceanic lithosphere subduction and orogenic belts are not randomly distributed but concentrated at two curvilinear trends on the earth, as shown in Figure 1a.

Wilson[4] first pointed out that the centers of curvatures of both island arcs and mountains along the Pacific Ocean lie on a great circle-like global rim (Figure 1a). In addition, centers of curvatures of convergence zones from the Mediterranean Sea through the Himalayas to the Tonga-Kermadec trenches nearly delineate a minor circle on the earth. The great and minor circles associated with the convergence zones presented by Wilson[4] cross obliquely each other at the South China sea region, where recent studies of mantle tomography[5] [6] [7] suggest the integration of relatively higher seismic velocity mass within the upper- and lower-mantle. It is likely that the integrated material of relatively higher seismic velocity has been supplied from plate subduction zones in the Southeast Asia.

To identify the fundamental characteristics of these circles associated with the global distribution of the subduction zones, studies confined to dynamics of the surface plates are insufficient. We also hypothesize that, to study the overall background of the global distribution of subduction zones, the great circle along the Pacific Ocean might be more important than the minor circle along the Mediterranean Sea to the Tonga-Kermadec trenches. The great circle presented by Wilson[4] suggests that, considering 3-D global downgoing flow regime, the major sites of energy dissipation associated with large-scale plate convergence process are generally distant from the trench axis, somewhere behind the axis. The trench axis might not be the most important component of the global lithosphere downgoing process but merely the initiation line for subduction. Eguchi[8] [9] proposed a concept of '*Cool Mantle Doughnut*' (hereafter, CMD) with the great circle dimension, inferred from previous studies, such as Wilson[4], and analyses of global seismic tomography and plate subduction history[10].

The CMD in Figure 1b may involve a zone of major energy dissipation associated not only with the plate convergence but also with the global mantle downwelling flow. The CMD corresponds to a global-scale zone of relatively lower temperature than average within the mantle layer behind the subduction zones surrounding the Pacific Ocean. The vertical cross section of the CMD outline might not be circular. The subduction zone bounds the shallowest oceanic rim of the CMD. The circumference-averaged centroid of the energy dissipation within the CMD might be within the lower mantle. The centroid depth might vary along the CMD, because of inhomogeneous dynamic processes along the circum-Pacific. Studies on paleo-subduction zone history[10] [11] [12] indicate that previous subduction zones surrounding the Pacific have been limited within the CMD with a lifetime $> 1 \times 10^2$ My (million years). Mathematically, the CMD would correspond to a function of *"bounded variation (BV)"* of major subduction zones surrounding the Pacific for at least the last 1×10^2 My. These studies[10] [11] [12] suggest that the CMD should be modeled as a weighted *BV* function at least for the last 10^2 Ma

because of the regionally dependent slab-supply history down to the lower mantle. Eguchi[9] also proposed a hypothetical concept of *'higher potential zone of subduction'* outlined by the CMD.

Thus, we can present a conceptual geodynamics theorem; the site of higher subduction potential defined by the great-circle-like CMD is a geometrical expression of Maupertuis' principle for large-scale downwelling flows within the mantle layer beneath the circum-Pacific region.

As demonstrated in numerical simulation studies[13) 14) 15) 16) 17)], phase transitions, such as those at 670 km depth, influence the evolution of 2-D or 3-D mantle convection. Other types of research[18) 19) 20)] have shown the predominant effect of surface plate motions on the global mantle flow regime. However, in this study, we focus primarily on simple cases of point or great-circle sources, although the drag forces due to surface plate motion or phase transitions may provide important dynamics that control mantle convection.

We will insert a great-circle source of relatively lower temperature to reveal the basic characteristics governing the subduction process. The great-circle source is an over-simplified model of large-scale subduction zone. Therefore, we neglect the effect of phase transitions as well as surface plate motions, because our main interest is focused on the Green function-like character of the dynamic response from an instantaneous anomaly appearing within the mantle layer.

2. Simulation of Mantle Convection

To investigate unsteady mantle flow dynamics, especially associated with the global subduction process, we developed a new code for 3-D numerical simulations of mantle convection. The code is applicable to flow problems with arbitrary time-space dependent thermal sources. The basic three equations concerning mantle convection are for continuity, motion with the Boussinesq (incompressible) approximation, and (thermal) energy conservation. Our simulation code can incorporate the 3-D spherical mantle layer with temperature- and pressure-dependent viscosity. In addition, we can set the viscosity model to be sensitive to the strain rate. Our program is based on the finite difference method with staggered grids. After the finite difference discretization process using basic equations with spherical polar coordinates, we obtain five equations that include three components, the velocity vector, pressure, and temperature. We followed the Newton method to obtain time integration with high precision. The Jacobian, due to the Newton method, for the five discretized equations is defined by the matrix composed of partial derivatives with the five individual arguments for the velocity vector, pressure, and temperature. The coefficient matrix of the simultaneous equations for the whole mantle after the application of the Newton method is filled with 5×5 small block matrices for finite difference volumes separated into mantle layer grids. Thus, the coefficient matrix to be solved numerically is sparse. The time step interval automatically becomes smaller for iterations with a complicated flow system to obtain accurate calculation results of mantle convection for a period of $\geq$ 10 My. To precisely calculate the sparse matrix associated with solving the five finite difference equations, we adopted an iterative method. Based on our experience using limited computer memory resources, the direct method for the mantle flow calculation does not yield a solution with higher accuracy. In more detail, we selected a preconditioned 'Bi-Conjugate Gradient Stabilized method' (hereafter, called preconditioned Bi-CGSTAB method) among several iterative techniques available. The Bi-CGSTAB method[21)] is currently known as one of the most useful techniques to obtain stable estimations of mathematically appropriate parameters with rapid convergence during the numerical iteration process. In comparison, an iterative calculation based on the Bi-CG (Bi-Conjugate Gradient) method has flaws such that the norm of the residual vector during the iteration does not decrease but oscillates intensively. Before applying the Bi-CGSTAB method, 'preconditioning' is required to attain rapid numerical convergence during the calculation because there are two problems in solving the simultaneous equations in the sparse coefficient matrix. First, the diagonal term for the continuity equation is zero. Second, the ratio of the non-diagonal terms against the diagonals reaches the

order of Rayleigh number, that is, the non-diagonal terms are large. The precondition, applied here, includes a matrix-matrix manipulation and incomplete LU factorization. The former is the multiplication by an inverse of a 5 × 5 block diagonal matrix, analytically derived using the original 5 × 5 small block matrix. To obtain a stable solution for finite difference volumes at the polar areas, we applied, for example, a low-pass filtering process. By incorporating the preconditioned BiCGSTAB method, we observed an improvement in both the computer memory consumption and convergence time during the calculation. We assigned the top- and bottom-boundary conditions of the velocity parameters to be slip and non-slip, respectively.

Table I. Model parameters for the mantle flow calculation in cases A to E.

Case	Grids (Lat., Radial)	η_0 (Pa s)	Cool Ring N-S Width (°)	Depth (km)
A	72, 24	10^{22}	< ±3.75	687.5
B	181, 24	10^{22}	< ±3.75	687.5
C	72, 24	(#)	< ±3.75	687.5
D	72, 24	10^{22}	< ±26.25	687.5
E	72, 24	10^{22}	(*)	687.5

(#) η_0 is 10^{20} for T > 3000 K, and 10^{22} for T < 3000 K.

(*) The same as in case A, in addition to gradually increasing temperature at 687.5 km from the equator to the poles.

Rheology parameters assumed were: thermal diffusivity = 1.0 x 10^{-6} [m^2 s^{-1}], coefficient of thermal expansion = 2.0 x 10^{-5} [K^{-1}], specific heat = 1.0 x 10^3 [J kg^{-1} K^{-1}]. Initial velocity is zero. (No internal heat source and no phase change.) Here, η_0 is the constant factor for temperature dependent viscosity. The latitudinal scale of the 'cool ring' at the equator, which is a simplified model of the circum-Pacific ocean subduction zone, is located at the boundary grid at 687.5 km, corresponding to the boundary between the upper- and lower-mantle in our model. The number of the longitudinal grids is four. The Rayleigh number is approximately 2.7 × 10^7. The Nusselt number near the surface is ~ 4.

According to the limited memory resources available on the super-computer at NIED (National Research Institute for Earth Science and Disaster Prevention), the grid distance of the 3-D spherical earth mantle cannot be set to values small enough to calculate realistic local dynamics. Here, possible examples of local dynamics are upwelling or downwelling flow conduits on the scale of ≤ 10 km. Therefore, our calculations reveal relatively large-scale phenomena concerning mantle convection.

After verifying the calculation accuracy of the program, we carried out several simulations to investigate the effects of lithosphere subduction along the circum-Pacific ocean during the last 100 My and other basic, elementary mantle flow processes. During our calculation, we imposed the initial condition of a zone of relatively lower temperature along the equatorial ring at the boundary between the upper and lower mantle, in the horizontally uniform thermal field. That is, for simplicity, we adopted a reference coordinate system that placed the CMD location at the equator. We introduced thermal boundary layers both within the upper-mantle and just above the core-mantle boundary. The depth range of the thermal boundary layers may depend on the grid division length because we set small temperature jumps between adjacent grids to calculate the physical parameters with high accuracy.

Figures 2 and 3 represent the initial temperature profiles for different simplified CMD models (cases A, B, C, D, and E). Model parameters, such as grid sizes for the cases in Figures 2 and 3, are given in Table I. Case B has double the number of latitudinal grids in comparison to those in basic case A. To confirm the viscosity layering within the mantle, we input model case C. In case D, the latitudinal width of the cool ring is the maximum, i.e., the ring is 52.5° wide across the equator, as shown in Table I. The anomaly of the thermal field imposed around 687.5 km in depth for case E is a function of the latitude; it is the highest at the poles and lowest at the equator, as shown in Figure 3. We included cases B, C, D, and E to analyze the size of the effect from changing the initial condition from the basic case A, i.e., the change in upwelling sites due to the downgoing cool mass. We set other model parameters as follows: mantle thickness is 3.0 × 10^3 km, radius of the earth is 6,291 km, surface density is 3.3 × 10^3 kg m^{-3}, and gravitational acceleration is 10 m s^{-2}. The other parameters are provided in

Table I. The viscosity of the mantle, η, is generally given as

$$\eta = \eta_0 \left[\varepsilon\right]^{\left[(1-n)/n\right]} \exp\left[\left(E^* + PV^*\right) / \left(RT\right)\right] \quad (1)$$

where η_0 is a constant, $[\varepsilon]$ is strain rate, E^* is activation energy, P is pressure, V^* is activation volume, R is the universal gas constant, and T is temperature. In this study, for simplicity, we assumed that n = 1, E^* = 4 J mol^{-1}, V^* = 0, R = 8.32 J mol^{-1} K^{-1}. Our model values of η_0 for cases A through E are provided in Table I.

In the mantle model, for simplicity, we did not incorporate any internal heat sources and phase change effects throughout the mantle layer. We start the calculation with zero initial velocity and displacement within the whole mantle layer.

3. Simulation Results

Because of fluid dynamics, the equatorial cool zone corresponding to the centroid of the downgoing lithosphere excites itself into downwelling mantle flow. As time progresses within the calculation, the deformation develops gradually over wider areas. The temporal development of the downgoing flow due to the cool mass induces the formation of upwelling sources near the core-mantle boundary with latitudinal distances of approximately 30°. The upcoming cells at the latitude of ~ 30° develop into large-scale upwelling flows which reach the earth's surface layer after 20 My in case A (shown in the temperature profile in Figure 4). The calculation results after certain periods of time for the other cases B, C, D, and E are provided in Figures 5, 6, 7, and 8, respectively.

The results (Table II) show that large-scale upwelling flows will exit at latitudes of 30 to 40°, after a certain period, in response to equatorial lithosphere subduction. The case of wider zone north-south of equatorial subduction can shift the upwelling sites to slightly higher latitudes than ~ 30°, as shown in Figure 6 (case C) and Figure 7 (case D). Due to relatively longer expenditure in computing time for case C to maintain a higher precision time integral, we plot the result 4 My in Figure 6. In Figure 6b, we can clearly observe the vertical velocity field in which the equatorial cool mass has already started moving into the lower mantle. In addition, a weak pattern of incipient upwelling flows has been subsequently progressing at the mid-latitudes in Figure 6b, although the thermal field in Figure 6a does not show a clear pattern of mature hot plumes. This indicates that the 4 My duration is too short to develop mature hot plumes.

Our results shown in Figures 4 to 8 suggest that it takes more than ~10 My to develop hot (and cool) thermal plumes due to subduction of an equatorially positioned cool ring near the top of the lower mantle inserted at 0 My. Case E, a latitudinal increasing field of the thermal anomaly initially inserted around 687.5 km depth, yields upwelling flows at a latitude of ~ 33°, as shown in Figure 8.

Table II. Comparison of the major upwelling flow sites in both the northern and southern hemispheres. These sites are excited by the down-welling of the equatorial cool ring, which was instantaneously settled at 687.5km depth within the initially static layered mantle. Results for different cases (A to E) are based on conditions shown in Table I.

Case	Approximate latitude of the two major upwelling rings (°)
A	30
B	30
C	40
D	40
E	33

A comparison of the major upwellings sites for case A (Figure 4) and case E (Figure 8) suggests that the increase in the latitudinal thermal anomaly with a total amplitude of approximately 200°, as defined in Table I and Figures 2 and 3, slightly shifts the latitudinal location of upwellings from ~ 30 (case A) to ~33° (case E). All cases from A through E show secondary down-flow systems at a latitude of ~ 60° and weaker upwelling at the polar-regions. Therefore, our simulation result has confirmed that the sites of large-scale major upwellings cannot directly reach the North and South poles.

Although the upwellings at the polar regions are weaker than those at ~ 30°, a relatively broad zone of upwelling flows at

higher latitudes, due to the equatorial cool source, could play an important role in more complicated dynamic regimes within the mantle.

4. Discussion

The slab supply down to the lower mantle from the circum-pacific ocean, which was modeled as CMD[8) 9)], can be interpreted as a global-scale down-flow system given the thermo-mechanic aspect of dynamics of the earth's interior. The concept of the CMD provided information for promoting or developing a new simulation code for a 3-D spherical shell of the mantle layer. The numerical simulation associated with the thermal image of CMD characterizes the elementary processes of large-scale mantle flows within the earth. The dynamic responses are upwellings from the core-mantle boundary that develop at ~30° distance from the initial instantaneous input of a cool ring mass below the equator. These represent the geometry of basic Green functions due to instantaneous input of thermal anomalies associated with the global mantle convection.

Here, it must be emphasized that the location of upwellings at the angle distance of ~30° originated from the initial instantaneous input of an equatorial cool ring source may be true only when the thermal structure of the mantle is uniform, as indicated in Figures 2 and 3. In the case of other *a priori* unstable thermal stratifications within the mantle, the simulation may result in patterns different than those in Figures 4 to 8. Our simulations with the given initial conditions cannot initiate the activity of local upwelling plumes at isolated localities even in the case of multiple longitudinal grids. This feature supports the validity of our numerical simulation code, because the scenario described is an axisymmetric problem.

Our calculation model yielded a mean descent rate of ~ 7 cm/y for a small equatorial cool block into the lower mantle. A recent study[22)] with different physical parameters in the lower mantle, such as the higher viscosity than in this study, showed a block of subducted oceanic lithosphere sinking with a speed of ~ 1 cm/y.

Thus far, we have not incorporated any effects of phase change, compositional mixing, or differentiation. Our basic calculation is not sufficient to initiate the activity of large-scale upwelling plume at isolated localities, as stated previously. To initiate and localize the large-scale mantle plume activity at isolated areas, other additional dynamical origins must be incorporated. For example, to excite major polar upwelling plumes in our model setting, pre-existing flows or other dynamics that attract rising plumes at the higher latitudes need to be superimposed. Similarly, to divide the zonal upwelling into several small plume activities at the latitude of ~ 30°, some additional dynamic source(s) at low latitudes are required. For example, to calculate such a complicated problem, a more realistic mantle viscosity profile and information on pre-existing flow system should be taken into account. Some aspects of the current mantle flow system might indirectly be inferred from reliable research on global seismic tomography. However, there is no convincing information on the pre-existing flow system, even for the current stage of the earth mantle. There are some lines of indirect information, such as that from global tomography study of the seismic velocity or seismic wave attenuation structure. To transform seismic structure information into mantle rheology parameters, such as temperature distribution and/or composition, at a minimum, a detailed convincing study on both up-to-date global seismology and mineral physics is necessary. Thus far, however, there has been some difficulty in identifying a realistic thermal structure of the mantle because even seismic tomography studies have been providing various models for P- and/or S- wave structure. Mineral physics studies of the mantle are also struggling to manifest a realistic structure of the mantle. Therefore, state of the art research on mantle temperature structure is still in its developing stage. This is one reason that in the initial conditions of the mantle model, we neglected the horizontal inhomogeneous structure except the instantaneous input of an anomalous temperature mass at a certain depth.

To reveal a more realistic response of the mantle flows due to global subduction zones, we should incorporate large-scale cooler sources from convergent-type plate boundaries in addition to the

circum-Pacific, including the Mediterranean Sea and Tonga-Kermadec. However, the degree of dynamic contribution from the latter might be smaller than from the former. In addition, the regimes of pre-existing flows, horizontal thermal gradients within the mantle, and effects of the mineral phase changes must be considered to excite localized upwelling plume activity. Moreover, we must numerically demonstrate the effect of unknown lateral flow dynamics at the lowermost mantle layer, i.e., D" layer, the most probably site of hot plume formation. Recently, Montague and Kellogg[23] demonstrated the effect of the D" layer as a dense basal boundary layer on mantle flows. Numerical simulations with the additional dynamic origins described previously are being partly conducted in a separate study[24].

5. Conclusions

To investigate the effect of the past circum-Pacific lithosphere subduction on the large-scale plume activity, we developed a new program code for mantle convection. The code is based on the finite difference method. We adopted the Newton method to precisely calculate the variable time step. The viscosity can be set to temperature-, strain rate- and/or pressure-dependence. The program incorporated the preconditioned Bi-CGSTAB method to, at each time step, precisely solving the sparse matrix of coefficients of the simultaneous equations constructed for the five scalar parameters of the velocity vector, pressure, and temperature. We then conducted basic simulations for five cases (A through E) of spherical flow patterns due to the equatorial cool ring, which was initially inserted at 687.5 km depth within the static layered mantle.

Our simulation result indicates that the large-scale upwellings occur at the latitudes of ±30~40° in response to the zonal downwelling flows due to the equatorial cool ring. In the case of a wider north-south cool ring (case D), we found the upwelling sites were at slightly higher latitude than 30°. Moreover, subsequent weak upwellings are obvious at the polar-regions. Although the model parameters used in this study are rather oversimplified, our simulation result may reveal part of the elementary processes of large-scale mantle flows within the terrestrial earth.

Acknowledgements

The numerical calculation in this study was primarily conducted on the super-computer at NIED (National Research Institute for Earth Science and Disaster Prevention, Tsukuba, Japan). This study was partly supported by a special coordination fund from STA (Science and Technology Agency) of Japan for promoting researches on 'whole-earth dynamics.'

References

1) S.K. Runcorn, "A growing core and a convective mantle," in *Isotopic and Cosmic chemistry*, North-Holland (1963), pp. 321-340.
2) S. Chandrasekhar, "Hydrodynamic and hydromagnetic stability," Oxford, (1961) p.652.
3) J.T. Ratcliff, G. Schubert, and A. Zebib, "Steady tetrahedral and cubic patterns of spherical shell convection with temperature-dependent viscosity," *Journal of Geophysical Research*, **101** (1996), pp. 25, 473-25,484.
4) J. T. Wilson, "*The Earth as a Planet*," edited by Kuiper, Univ. Chicago Press, **III** (1954), p.138.
5) Y. Fukao, M. Obayashi, H. Inoue, and M. Nenbai, "Subducting slabs stagnant in the mantle transition zone," *Journal of Geophysical Research*, **97** (1992), pp. 4,809 - 4,822.
6) R. D. Van der Hilst, S. Widiyantoro, and E. R. Engdahl, "Evidence for deep mantle circulation from global tomography," *Nature*, **386** (1997), pp. 578 – 584.
7) G. Masters, G. Laske, H. Bolton and A. M. Dziewonski, "The relative behavior of shear velocity, bulk sound speed, and compressional velocity in the mantle – implications for chemical and thermal structure," in *Earth's Deep Interior – Mineral Physics and Seismic Tomography*, edited by Karato, S., A. M. Forte, R. C. Liebermann, G. Masters and L. Stixrude, Am. Geophys. Uni. (2000).
8) T. Eguchi, "Dynamics due to "the Cool Mantle Doughnut," *Programme and Abstracts of Seismol. Soc. Japan*, No.2, (1993), pp.351-351.
9) T. Eguchi, "Dynamics due to Cool Mantle Doughnut" (abstract), *Eos*

Trans, Am. Geophys. Uni. **75**, 44 suppl. (1994), pp.67-67.
10) M. A. Richards and D. C. Engebretson, "Large-scale mantle convection and the history of subduction," *Nature*, **355** (1992), pp.437-440.
11) C. Lithgow-Bertelloni and M. A. Richards, "The dynamics of Cenozoic and Mesozoic plate motions," *Reviews of Geophysics* **36** (1998), pp.27-78.
12) R. D. Müller, M. Sdrolias, C. Gaina and W. R. Roest, "Age, spreading rates, and spreading asymmetry of the world's ocean crust," *Geochemistry, Geophysics, Geosystems*, **9**[4] (2008), doi: 10.1029/2007GC001743.
13) G. Schubert and D. L. Turcotte, "Phase changes and mantle convection," *Journal of Geophysical Research*, **76** (1971), pp. 1,424-1,432.
14) U. R. Christensen and D. A. Yuen, "Layered convection induced by phase transitions," *Journal of Geophysical Research*, **90** (1985), pp. 10,291-10,300.
15) S. Honda, D. A., Yuen, S. Balachandar, and D. Reuteler, "Three-dimensional instabilities of mantle convection with multiple phase transitions," *Science*, **259** (1993), pp. 1308-1311.
16) P. J. Tackley, "On the penetrations of an endothermic phase transition by upwellings and downwellings," *Journal of Geophysical Research*, **100** (1995), pp. 15,477-15,488.
17) Y. Iwase, "Three-dimensional infinite Prandtl number convection in a spherical shell with temperature-dependent viscosity," *Journal of Geomagnetism Geoelectricity* , **48** (1996), pp. 1,499-1,514.
18) G. F. Davies, "Role of lithosphere in mantle convection," *Journal of Geophysical Research,* **93** (1988), pp. 10,451-10,466.
19) H.-P. Bunge and M.A. Richards, "The origin of large scale structure in mantle convection: effects of plate motions and viscosity stratification," *Geophysical Research Letters,* **23** (1996), pp. 2,987-2,990.
20) S. Zhong, M.T. Zuber, L. Moresi and M. Gurnis, "Role of temperature-dependent viscosity and surface plates in spherical shell models of mantle convection," *Journal of Geophysical Research*, **150** (2000), pp. 11,063-11,082.
21) H. A. Van der Vorst, "Bi-CGSTAB: A fast and smoothly converging variant of Bi-CG for the solution of nonsymmetric linear systems," *SIAM Journal on Scientific and Statistical Computing*, **13**[2] (1992), pp. 631 - 644.
22) H. C˘íz˘ková, A. P. van den Berg, W. Spakman and C. Matyska, "The viscosity of Earth's lower mantle inferred from sinking speed of subducted lithosphere," *Physics of the Earth and Planetary Interiors,* **200–201** (2012) pp. 56–62.
23) N. L. Montague and L.H. Kellogg, "Numerical models of a dense layer at the base of the mantle and implications for the geodynamics of D"," *Journal of Geophysical Research*, **150** (2000), pp. 11,101-11,114.
24) T. Eguchi, K. Matsubara and M. Ishida, "Three-dimensional dynamic response functions of instantaneous input of localized and large-scale zonal thermal anomalies into the static layered mantle," *in preparation* 2017.

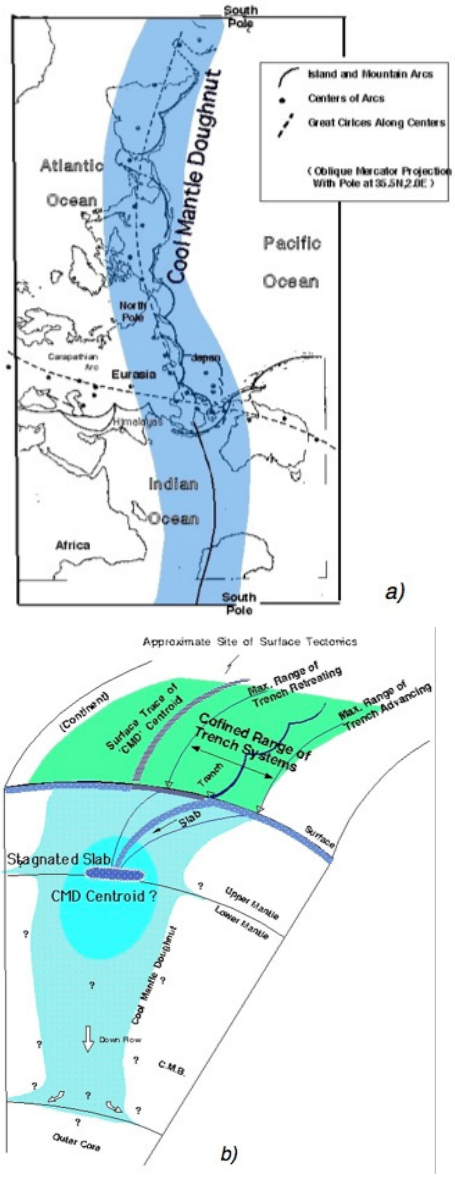

Figure 1. *a)* Hypothesized map of *'Cool Mantle Doughnut'* (CMD) [8) 9)] on a map of centers of both islands and mountains arcs being traced approximately by a great circle (modified from Wilson[4)]) on the earth. In this map, studies of seismic tomography as well as lithosphere subduction history[10)] etc. were taken into account. CMD is represented as a shaded area.
b) Schematic vertical cross-section view of CMD.

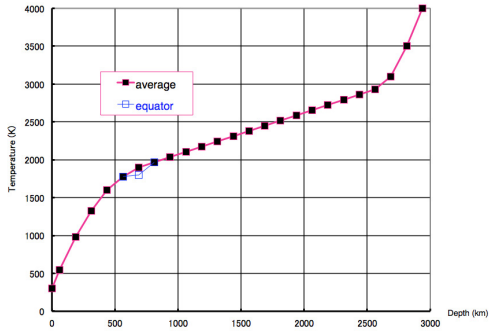

Figure 2. Profile of the initial temperature field for calculation of the 3-D spherical mantle layer, including the 'equatorial cool ring' at 687.5 km depth for cases A, B, C and D shown in Table I. Here, the equatorial cool ring, where the temperature is 100 deg. lower than the surrounding mantle, is an over-simplified model of the circum-Pacific ocean subduction. No phase change and no internal heating are incorporated.

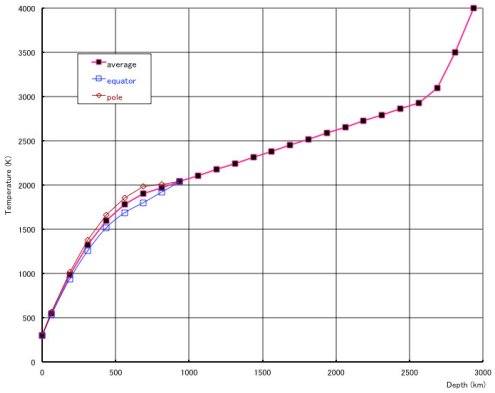

Figure 3. Profile of the initial temperature field for case E shown in Table I. The thermal field imposed around the 687.5 km depth is the highest at the poles and the lowest at equator. The else is the same as in Figure 2.

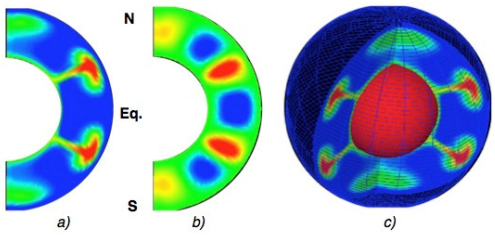

Figure 4. Cross-section view of the result of mantle flow simulation for case A defined in Table I and Figure 2, at the calculation time of 20 My. a) North-south vertical section of the thermal field. (Red = hotter, Blue = cooler.) b) N-S vertical cross-section of the radial velocity field. (Red = upwelling, Blue = downgoing.) c) Spherical cross-section image of the thermal field.

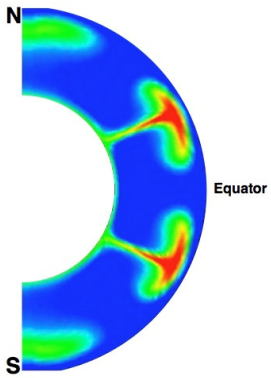

Figure 5. North (top)-South (bottom) cross-section of the thermal field of the mantle for case B defined in Table I and Figure 2, at the calculation time of 25 My. (Red = hotter, Blue = cooler.)

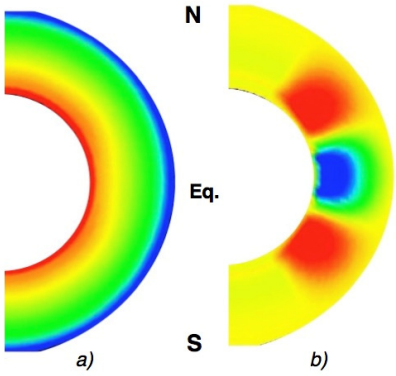

Figure 6. Cross-section of the result of mantle flow simulation for case C described in Table I and Figure 2, at the calculation time of 4 My. The colors of a) and b) are the same as in Fig. 4.

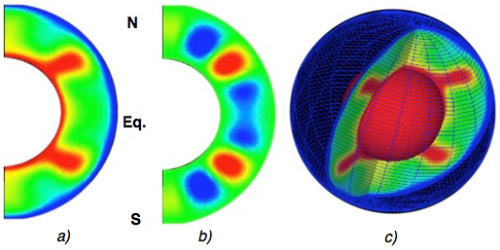

Figure 7. Cross-section of the result of mantle flow simulation for case D defined in Table I and Figure 2, at the calculation time of 15 My. The others of a), b) and c) are the same as in Fig. 4.

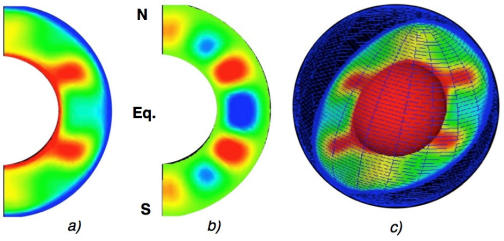

Figure 8. Cross-section of the result of mantle flow simulation for case E shown in Table I and Figure 3, at the calculation time of 16 My. The others of a), b) and c) are the same as in Fig. 4.